Localized and Cellular Patterns in a Vibrated Granular Layer

Lev S. Tsimring[1] and Igor S. Aranson[2,3]
[1]*Institute for Nonlinear Science, University of California, San Diego, La Jolla, California 92093-0402*
[2]*Department of Physics, Bar Ilan University, Ramat Gan 52900, Israel*
[3]*Argonne National Laboratory, 9700 Cass Avenue, Argonne, Illinois 60439*
(Received 26 March 1997)

We propose a phenomenological model for pattern formation in a vertically vibrated layer of granular material. This model exhibits a variety of stable cellular patterns, including standing rolls and squares as well as localized objects (*oscillons* and *worms*), similar to recent experimental observations [Umbanhowar, Melo, and Swinney, Nature (London) **382**, 793 (1996)]. The model is an amplitude equation for the parametrical instability coupled to the mass conservation law. The structure and dynamics of the solutions resemble closely the properties of localized and cellular patterns observed in the experiments. [S0031-9007(97)03534-5]

PACS numbers: 47.54.+r, 46.10.+z, 47.35.+i, 81.05.Rm

Granular materials exhibit a unique mixture of properties of both liquids and solids [1]. Intensive theoretical, numerical, and experimental studies of granular systems revealed a wide variety of new phenomena typical for granular systems, such as clustering and inelastic collapse [2], random force chains [3], granular convection [4], and cellular patterns in vibrated layers [5–7]. The very complicated rheology of granular media makes their theoretical analysis extremely difficult. Unlike fluid dynamics, there is no reliable continuum description of a granular system applicable in a wide range of conditions. The widely used approach is a straightforward simulation of many interacting particles in a gravity field [8,9].

Vibrated granular systems often manifest fluidlike behavior which resembles similar phenomena in conventional liquids. Recent experimental studies of vertically vibrated granular systems [5–7] demonstrated a rich variety of collective behavior ranging from standing waves, hexagons, and squares to localized objects (particlelike *oscillons* [6] and one-dimensional *worms*, see [1]). Cellular patterns are remarkably similar to Faraday waves in fluids [10] which have recently been a subject of intensive research (see, e.g., [11]). The difference, however, is that the primary bifurcation to square patterns and oscillons is hysteretic; patterns disappear at less magnitude of the plate vibrations than they first appear. The localized objects, oscillating at half frequency of plate vibrations $\Omega/2$ on the background of a flat surface oscillating at Ω, are observed in slightly subcritical parameter region for cellular patterns. In this Letter we propose a simple continuum model exhibiting phenomenology remarkably similar to the experimental observations. Due to its simplicity, it is amenable to a comprehensive analysis. Although this model is not derived from the corresponding microscopic equations of granular systems, it is instructive for interpretation of experimental data and may yield testable predictions.

The model consists of an amplitude equation for the order parameter ψ coupled to a conservation law for an average mass of granular material per unit area (or a local averaged thickness of the layer):

$$\partial_t \psi = \gamma \psi^* - (1 - i\omega)\psi + (1 + ib)\nabla^2 \psi - |\psi|^2 \psi - \rho\psi, \tag{1}$$

$$\partial_t \rho = \alpha \nabla \cdot (\rho \nabla |\psi|^2) + \beta \nabla^2 \rho\,. \tag{2}$$

Equation (1) without the last term is a popular model for the parametric instability in oscillating liquid layer (see [13,14]). The order parameter $\psi(x, y, t)$ characterizes local complex amplitude of the particle oscillations at the frequency $\omega = \Omega/2$. Linear terms in this equation can be derived from the dispersion relation for parametrically driven granular waves, expanded near frequency ω and corresponding wave number k (here $k = \sqrt{\omega/b}$, parameter b must chosen to reproduce the correct wave number at a given frequency). The term $\gamma\psi^*$ provides parametric driving and leads to the excitation of standing waves. The term $|\psi|^2\psi$ phenomenologically accounts for the nonlinear saturation of oscillations provided in granular materials by restitution. The last term in Eq. (1) accounts for the coupling of the order parameter to the local average density ρ. As it is observed experimentally [5,6], the threshold value of the vibration amplitude γ for the parametric instability depends on the mean layer thickness [5] due to an increase of internal energy dissipation in thicker layers. Although one should generally expect this term to be $f(\rho)\psi$ with $f(\rho)$ saturating at large ρ (when the thickness of the layer is larger than the scale of typical perturbations), we hereafter limit ourselves with the simplest form $f(\rho) = \rho$ corresponding to relatively thin layers (proportionality constant can be omitted after appropriate scaling of ρ). Equation (2) describes the conservation of the granular material. Two different physical mechanisms contribute to the in-plane mass flux. The first term in (2) reflects the average particle drift due to the gradient of magnitude of high-frequency oscillations. On average, particles try to "escape" from regions of large fluctuations, the

effect analogous to the formation of so-called Chladni figures [12]. The second term describes diffusive relaxation of the inhomogeneous mass distribution. We expect the effective "granular temperature" and corresponding diffusion constant β to be proportional to the energy of plate vibrations, and then for nonvibrating plate the diffusion constant turns to zero and an arbitrary pattern "freezes".

Let us briefly discuss the linear stability properties of Eqs. (1) and (2). The trivial state $\psi = 0$, $\rho = \rho_0$ corresponding to a flat layer becomes unstable at $\gamma^2 = \gamma_c^2 = [\omega + b(1 + \rho_0)]^2/(1 + b^2)$ for $\omega b > 1 + \rho_0$ with respect to a periodic perturbations with the wave number k_c given by $k_c^2 = (\omega b - 1 - \rho_0)/(1 + b^2)$. For $\omega b < 1 + \rho_0$ spatially uniform perturbation with $k_c = 0$ become unstable first, and the vibration threshold is $\gamma_c^2 = 1 + \rho + \omega^2$. Due to the rotational invariance of (1) and (2), waves with all directions grow simultaneously.

Above the threshold, the nonlinear terms in Eqs. (1) and (2) saturate the exponential growth of perturbations and provide pattern selection. The problem of pattern selection requires careful analysis of patterns with different symmetries. For $\rho = \text{const}$, Eqs. (1) and (2) reduce to a single equation for which it is known that rolls are the only stable cellular pattern above onset [13]. This has been a serious shortcoming of this model since square patterns are frequently observed in Faraday experiments [5,11]. Usually pattern selection depends sensitively on the choice of nonlinearity in the model, and some tweaking with nonlocal nonlinearities could remedy this problem (see, e.g., [15]). It turns out that within our combined model with ρ being a dynamical variable it is not needed; squares and rolls emerge naturally in different parameter regions.

Consider stability of simplest cellular patterns (rolls and squares) in the framework of Eqs. (1) and (2) close to the threshold of parametric instability. Although the analysis is formally valid for arbitrary rhombic pattern, we restrict ourselves to the squares since they are typically preferred by the symmetry. Within the framework of weakly nonlinear analysis (small supercriticality ε defined below), cellular patterns are described by the following solution to Eq. (1):

$$\psi = [A \sin(k_c x) + B \sin(k_c y)]e^{i\phi} + w, \qquad (3)$$

where $A(t)$, $B(t)$ are the real amplitudes of two (orthogonal) standing waves, phase $\phi = \text{const}$ is given by the solution of the linearized problem, and w is a correction to the solution which we demand to be small at $\varepsilon \to 0$. Near the threshold the density ρ is enslaved to $|\psi|^2$, and follows the quasistationary solution of Eq. (2), $\rho = \rho_0(t) \exp[-\eta|\psi|^2]$, $\eta = \alpha/\beta$. The function $\rho_0(t)$ can be found from the condition of total mass conservation $S^{-1} \int \rho dx dy = \mu = \text{const}$, S is the total area. Substituting ρ into Eq. (1) and performing standard orthogonalization procedure to keep w small, we obtain the following equations for $A(t)$, $B(t)$ (for simplicity we retain nonlinearity only in two first orders):

$$\dot{A} = A\left[\varepsilon + \frac{\mu\eta - 3}{4} A^2 + \frac{2\mu\eta - 3}{2} B^2 - \frac{\mu\eta^2}{2}(B^2A^2 + 2B^4)\right]. \qquad (4)$$

The equation for $B(t)$ is obtained by the permutation $A \Leftrightarrow B$. The supercriticality parameter is given by $\varepsilon = \gamma_c(\gamma - \gamma_c)/(1 + \mu + k_c^2)$ [16]. It follows from Eq. (4) that hysteretic transition to squares ($A = B$) occurs if $\mu\eta > 9/5$ and stripes ($A \neq 0$, $B = 0$ or $A = 0$, $B \neq 0$) exhibit subcritical bifurcation at $\mu\eta > 3$.

In the supercritical case we can drop the last two terms in Eq. (4). It is easy to verify that for $\varepsilon \to +0$ the square pattern ($A = B$) is stable for $\mu\eta > 1$ and unstable otherwise. Rolls, in the limit $\varepsilon \to +0$, are stable for $\mu\eta < 1$ and unstable otherwise. For larger $\varepsilon > 0$ the higher order terms in Eq. (4) become important, and squares are stable at $16\mu\varepsilon\eta^2 < 3(10\varepsilon\eta - \varepsilon^2\eta^2 - 9)$ and rolls are stable at $4\mu\varepsilon\eta^2 > 3(\varepsilon\eta - \varepsilon^2\eta^2 - 3)$. In the subcritical case $\eta\mu > 9/5$ squares are stable in their entire basin of existence given by the condition $48\mu\varepsilon\eta^2 + (5\eta\mu - 9)^2 = 0$. The phase diagram for roll and squares in shown in Fig. 1. It is qualitatively consistent with the experimental observations of transition from rolls to squares with decreasing the driving frequency if one assumes that $\eta\mu$ decreases with an increase of frequency. One expects that the relative effect of particle drift from regions of intense fluctuations characterized by parameter η diminishes with the increase of ω since characteristic vertical scale of the layer involved in oscillations becomes smaller at high frequencies. At large positive ε there is a bistable region where rolls and squares coexist, also in agreement with experiments [5]. It should be noted, however, that the phase diagram of Eq. (4) exactly corresponds to the original model (1) and (2) only in the limit of small amplitude; otherwise it represents only a Galerkin approximation of the exact solution. Still, our numerical simulations agreed fairly well with these stability limits.

Now we consider the localized solutions. In experiments [6] oscillons appear slightly below the threshold

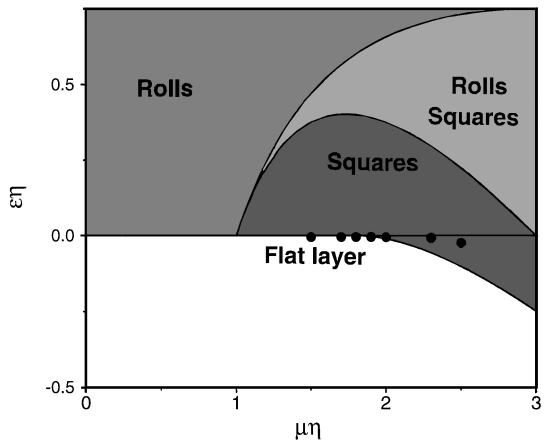

FIG. 1. Phase diagram for square and roll patterns, weakly nonlinear theory. Black dots indicate stable oscillons seen in numerical experiments.

of the parametric instability for cellular patterns. We also found stationary localized axisymmetric solutions to Eqs. (1) and (2) in weakly subcritical region (dots in Fig. 1 correspond to stable localized solutions found for various combinations of parameters). Figure 2 shows the radial structure of the order parameter ψ and corresponding distribution of ρ for such solution. This solution corresponds to a dip in the average mass distribution $\rho = \rho_0 \exp(-\eta|\psi|^2)$. Because of the symmetry $\psi \to -\psi$, oscillons of opposite polarities may coexist in this system. It has oscillating tails at $r \gg 1$, $\psi(r) \propto r^{-1/2}\exp(pr)$ with the (complex) exponent p given by $p^2 = -k_c^2 + \sqrt{(\gamma^2 - \gamma_c^2)/(1 + b^2)}$.

We studied the linear stability of those localized solution with respect to axisymmetric (usually the most dangerous) perturbations. Some of the results are presented in Fig. 3, where we show the largest eigenvalue of the linearized system λ, $|\psi(0)|$, and the mass deficit $m = 2\pi\rho_0(\int_0^\infty r \exp[-\eta|\psi|^2]dr - 1)$. The stability region is limited both at large and small γ in accord with experiments. At the edges of the stable region, $\gamma_{c1,2}$, the stable solution corresponding to the oscillon annihilates with other unstable localized solutions.

The interaction of two oscillons can be considered in the spirit of Ref. [17]. Since the asymptotic behavior of ψ for the oscillon is oscillatory with z, the interaction force $F \sim \mathrm{Re}\exp(pr)$ is oscillatory too. It is natural to expect a variety of bound states. A numerically found bound state of two oscillons with opposite phases is shown in Fig. 4(a), and a bound state of four oscillons (one positive surrounded by three negative) is shown in Fig. 4(b). As in the experiment [6] we found that bound states with coordination numbers higher than three are unstable. There also exist a stable bound state of two like-phased oscillons, but the equilibrium distance between the oscillons is substantially larger than for oppositely phase pairs, resulting in much weaker binding. Small "granular noise" probably unbinds such weakly coupled pairs.

We studied the nonlinear evolution of oscillons beyond their region of stability in numerical simulations of Eqs. (1) and (2). Once the lower bound γ_{c1} is passed, the oscillon rapidly decays toward a trivial state $\psi = 0$. Increasing γ above γ_{c2}, the instability leads to a range of different scenarios, depending on other parameters η, μ, ω, and α. For small $\eta\mu$ (supercritical transition) oscillons produces a sequence of concentric rolls. Depending on $\eta\mu$ they either remain rolls or break to produce a disordered square pattern. At larger $\eta\mu$ oscillon produces other oscillons on its periphery as seen in experiments [6]. It turns out, surprisingly, that the following oscillons do not appear uniformly around the center, but rather organize themselves in chains, resembling worm-like patterns [Fig. 4(c)], cf. photo by P. Umbanhowar published in [1]. We propose an explanation of this effect by the conservation of total mass. Oscillons push the granular material on their periphery. Since the excessive mass from oscillons in a chain is redistributed by the diffusion, it spreads more rapidly near the tip of the chain. Therefore, the next oscillon will likely appear there, and the tip advances (compare with diffusion-limited growth [18]). This process will continue until the average density in the surrounding flat regions becomes so high that the creation of new oscillons is halted (the threshold for oscillon stability γ_{c2} increases with the average density). Our simulations show that for values of γ slightly above γ_{c2} even after a long time, oscillons do not fill the entire area [see Fig. 4(d)].

Let us now return briefly to the problem of selection of cellular patterns. In the domain of oscillon stability, these patterns can be considered as a periodic lattice of weakly coupled oscillons. As it is well known from the solid-state physics, the lowest energy configuration of like-charged objects is a hexagonal lattice (compare with Abrikosov lattice). In contrast, for alternatively charged particles the optimal configuration is a square lattice where a positively charged particle is surrounded by four negatively charged (antiferromagnetic lattice). Equations (1) and (2) preserve the symmetry $\psi \to -\psi$, and therefore square patterns formed by both positive and negative oscillons dominate

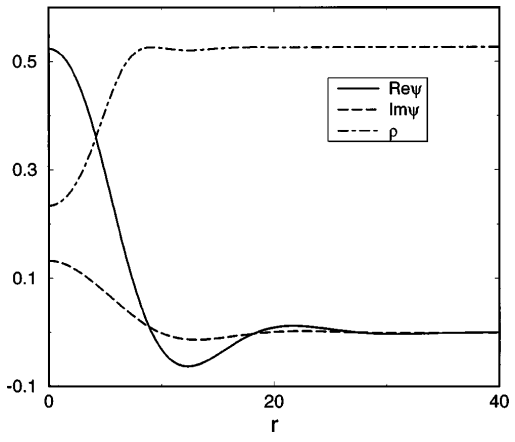

FIG. 2. Radial structure of the stable oscillon for $\gamma = 1.8$, $\mu = 0.527$, $b = 2$, $\omega = \alpha = 1$, and $\eta = 5/\gamma$.

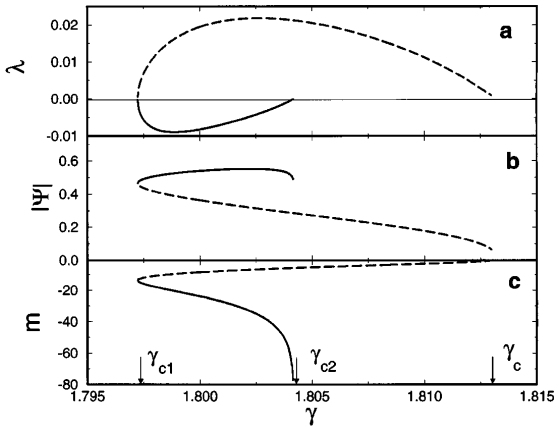

FIG. 3. Largest eigenvalue λ (a), $|\psi|$ at $r = 0$ (b), and mass deficit m (c) for stable (solid line) and unstable (dashed line) oscillons; $\mu = 0.527$, $b = 2$, $\omega = \alpha = 1$ and $\eta = 5/\gamma$.

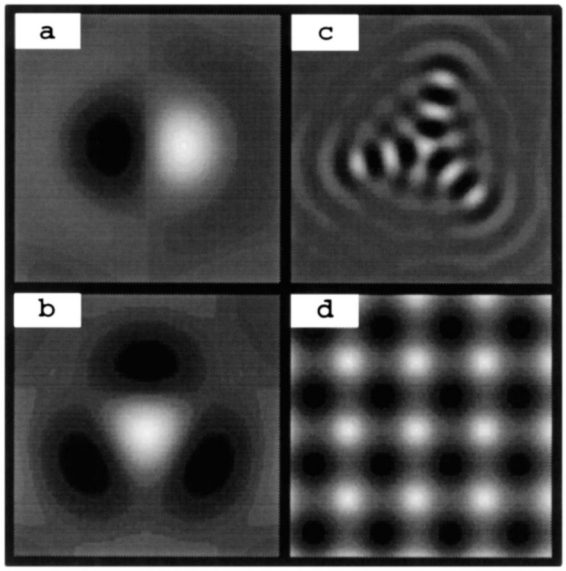

FIG. 4. Gray-coded images of Reψ (black corresponds to maximum, white to minimum) from simulations of Eqs. (1)–(2), (a) bound state of oppositely phase oscillons, $\alpha = \omega = 1$, $b = 2$, $\eta = 2.78$, $\mu = 0.527$, $\gamma = 1.8$, and size $L = 40$; (b) Triangular bound state, same parameters; (c) wormlike structure produced by a single oscillon in the center, $\alpha = 1$, $\omega = b = 2$, $\gamma = 2.245$, $\eta = 4.38$, $\mu = 0.525$, and $L = 100$; (d) square lattice, $\omega = \alpha = 1$, $\gamma = 1.84$, $\mu = 0.52$, $\eta = 2.72$, and $L = 100$.

[see Fig. 4(d)]. Once they symmetry is broken (as in two frequency driving), patterns are formed by like-phased oscillons, and the hexagonal symmetry can be expected. The selection of the pattern in the supercritical case where oscillons are unstable is more subtle. The advantage of the square pattern over rhombi cannot be determined in the lowest order of our weakly nonlinear perturbation theory, which happens to be insensitive to the angle between two standing waves. Our arguments related to optimal packing of localized structures suggest that the unique selection of square patterns should occur in higher order of ε.

We have shown on the basis of phenomenological model that the constraint of mass conservation plays a crucial role in pattern formation in vibrated granular materials. The parameters of the model can be estimated experimentally or from molecular dynamics. We can speculate that our results are also relevant for fluids, where square patterns are ubiquitous and localized objects were observed recently [19]. Parametric waves on a fluid surface induce mean surface displacement, which must obey a conservation law. Thus, we expect that a coupled set of equations for the order parameter and a mean displacement may serve as a paradigm model for this system. Although for fluids the knowledge of the Navier-Stokes equations allows for the direct stability analysis of cellular patterns [20], finding a relevant order-parameter model would be useful for studies of more complicated pattern formation in this rich experimental system. Wormlike structures have also been recently observed in electroconvection [21]. It is plausible to assume that as in a granular system, this effect can also be interpreted as the growth in a system, exhibiting a first-order transition to a cellular structure and controlled by a slowly diffusing field.

We thank M. I. Rabinovich, M. Mungan, H. L. Swinney, P. Umbanhowar, and H. Levine for illuminating discussions. This work was supported by the U.S. Department of Energy under Contracts DE-FG03-96ER14592 and DE-FG03-95ER14516 (L. T.) and W-31-109-ENG-38 (I. A.). The work of I. A. was also supported by NSF, Office of Science and Technology Center under Contract No. DMR91-20000.

[1] H. M. Jaeger, S. R. Nagel, and R. P. Behringer, Rev. Mod. Phys. **68**, 1259 (1996).
[2] I. Goldhirsh and G. Zanetti, Phys. Rev. Lett. **70**, 1619 (1993); F. Spahn *et al.*, Phys. Rev. Lett. **78**, 1596 (1997); A. Kudrolli, M. Wolpert, and J. Gollub, Phys. Rev. Lett. **78**, 1383 (1997); S. McNamara and W. R. Young, Phys. Rev. E **50**, R28 (1994); Y. Du, L. Hao, and L. P. Kadanoff, Phys. Rev. Lett. **74**, 1268 (1995).
[3] S. N. Coppersmith *et al.*, Phys. Rev. E **53**, 4673 (1996); F. Radjai *et al.*, Phys. Rev. Lett. **77**, 274 (1996).
[4] J. B. Knight, H. M. Jaeger, and S. R. Nagel, Phys. Rev. Lett. **70**, 3728 (1993).
[5] F. Melo, P. Umbanhowar, and H. L. Swinney, Phys. Rev. Lett. **72**, 172 (1994); *ibid* **75**, 3838 (1995).
[6] P. Umbanhowar, F. Melo, and H. L. Swinney, Nature (London) **382**, 793 (1996).
[7] E. Clement *et al.*, Phys. Rev. E **53**, 2972 (1996).
[8] G. H. Ristow and H. J. Herrmann, Phys. Rev. E **50**, R5 (1994).
[9] S. Luding *et al.*, Europhys. Lett. **36**, 247 (1996); K. M. Aoki and T. Akiyama, Phys. Rev. Lett. **77**, 4166 (1996).
[10] M. Faraday, Philos. Trans. R. Soc. London **52**, 299 (1831).
[11] See, e.g., A. B. Ezersky *et al.*, Sov. Phys.-JETP **64**, 1228 (1986); N. B. Tufillaro, R. Ramshankar, and J. P. Gollub, Phys. Rev. Lett. **62**, 422 (1989); S. Ciliberto, S. Douady, and S. Fauve, Europhys. Lett. **15**, 23 (1991).
[12] Chladni figures occur due to nonuniform external vibrations, and here the nonuniformity of oscillations is dynamical.
[13] W. Zhang and J. Vinals, Phys. Rev. Lett. **74**, 690 (1995).
[14] S. V. Kiyashko *et al.*, Phys. Rev. E **54**, 5037 (1996).
[15] M. Cross and P. C. Hohenberg, Rev. Mod. Phys. **65**, 851 (1993).
[16] Note that there are other $O(A^5, B^5)$ terms in Eq. (4) which come from the coupling of the primary waves with their high-order harmonics. However, these terms are small for high internal friction ($\mu \ll 1$, $\eta \gg 1$).
[17] I. S. Aranson *et al.*, Physica D **43**, 436 (1990).
[18] Eqs. (1)–(2) are reminiscent of phase-field models of dendrite growth; see, e.g., J. S. Langer, *Models of Pattern Formation in First-Order Phase Transitions* (World Scientific, Singapore, 1986).
[19] O. Lioubashevsky, H. Arbell, and J. Fineberg, Phys. Rev. Lett. **76**, 3959 (1996).
[20] P. Chen and J. Viñals (to be published).
[21] M. Dennin, G. Ahlers, and D. S. Cannell, Science **272**, 388 (1996).